



Published in final edited form as:

Nat Cell Biol. 2011 April ; 13(4): 383–393. doi:10.1038/ncb2216.

Analysis of the myosinII-responsive focal adhesion proteome reveals a role for β -Pix in negative regulation of focal adhesion maturation

Jean-Cheng Kuo^{1,**}, Xuemei Han^{2,**}, Cheng-Te Hsiao³, John R. Yates III^{2,*}, and Clare M. Waterman^{1,*}

¹Cell Biology and Physiology Center, National Heart, Lung, and Blood Institute, NIH, Bethesda, MD 20892

²Cell Biology, Scripps Research Institute, La Jolla CA 92037

³Proteomics and Analytical Biochemistry Unit, Research Resources Branch, National Institute on Aging, NIH, Baltimore, MD 21224

Abstract

Focal adhesions (FAs) undergo myosinII-mediated maturation wherein they grow and change composition to modulate integrin signaling for cell migration, growth and differentiation. To determine how FA composition is modulated by myosinII activity, we performed proteomic analysis of isolated FAs and compared protein abundance in FAs from cells with and without myosinII inhibition. We identified FA 905 proteins, 459 of which changed in FA abundance with myosinII inhibition, defining the myosinII-responsive FA proteome. FA abundance of 73% of proteins was enhanced by contractility, including those involved in Rho-mediated FA maturation and endocytosis- and calpain-dependent FA disassembly. 27% of proteins, including those involved in Rac-mediated lamellipodial protrusion, were enriched in FA by myosinII inhibition, establishing for the first time negative regulation of FA protein recruitment by contractility. We focused on the Rac guanine nucleotide exchange factor, β -PIX, documenting its role in negative regulation of FA maturation and promotion of lamellipodial protrusion, FA turnover to drive cell migration.

Integrin-mediated focal adhesions (FAs) are dynamic, multifunctional organelles that facilitate cell adhesion, force transmission and cytoskeleton regulation, as well as signaling that controls cell division, differentiation, or apoptosis^{1,2}. The diverse FA functionality is reflected in their complex composition. Over 150 different proteins are known to associate with FAs making up the “Integrin Adhesome”³. The Adhesome includes cytoskeletal-binding and adapter proteins and enzymes including kinases, phosphatases, phospholipases

Users may view, print, copy, download and text and data- mine the content in such documents, for the purposes of academic research, subject always to the full Conditions of use: http://www.nature.com/authors/editorial_policies/license.html#terms

*correspondence to: Clare M. Waterman (watermancm@nhlbi.nih.gov). John R. Yates III (jyates@scripps.edu).
**equal author contribution

AUTHOR CONTRIBUTIONS

J.C.K. and C.M.W. designed experiments and wrote the paper; J.C.K. performed experiments, X.H. and J.R.Y. performed MudPIT MS analysis; C.T.H. created the web site.

and small GTPases and their modulators. Furthermore, FA composition is heterogeneous and dynamic, even across different FAs within a single cell⁴. However, no FA compositions have been ascribed to specific downstream functions.

One important regulator of FA composition is physical perturbation^{5,6}. FAs are mechanosensitive and recruit proteins to grow, and change composition in response to tension in the process of FA maturation⁷⁻⁹. Tension driving FA maturation is supplied either by myosinII activity or external forces applied to the cell^{9,10}. Forces on tension-sensitive FA proteins drive conformational changes that unmask binding sites for non-tension-sensitive proteins¹¹. Thus, tension-mediated protein recruitment regulates FA composition to mediate outcome determination downstream of integrin-mediated adhesion¹².

The cascade of FA compositional changes during myosinII-mediated FA maturation is being elucidated for a small fraction of the Adhesome. After integrin activation by talin¹³, the adapter paxillin and the tyrosine kinase FAK are recruited to nascent FA¹⁴⁻¹⁶. FA growth is accompanied by recruitment of vinculin^{17,18}, which strengthens the integrin–talin-actin link^{19,20}. This is followed by formin-mediated elongation of an actin/ α -actinin bundle, where adapter proteins zyxin and tensin accumulate^{9,17,21}. Tension on integrins also promotes FAK and Src activation^{22,23} which phosphorylate tyrosines on paxillin and p130cas forming binding sites for SH2 domain-containing proteins²⁴. However, major differences in biological response downstream of integrin engagement are likely mediated by more significant FA compositional changes. Here, we utilized proteomic analysis to characterize FA composition changes induced by myosinII inhibition. We find myosinII mediates major compositional changes in FA. We focus on a Rac1 guanine nucleotide exchange factor (GEF), β -Pix whose FA abundance was enhanced by myosinII inhibition and demonstrate its role in negative regulation of FA maturation by promoting Rac1 activation, lamellipodial protrusion, and nascent FA turnover.

RESULTS

Development and validation of an FA isolation method

To characterize FA composition and its modification by myosinII activity, we developed a FA isolation method for HFF1 fibroblasts, minimizing contamination by actin stress fibers²⁵ (Fig. 1a). Cells were hypotonically shocked and strongly triturated to remove cell bodies and majority of the cytoskeleton, leaving substrate-bound FAs, together with a subset of thin and/or fragmented stress fibers for collection and analysis. Imaging cells expressing GFP-paxillin during hypotonic shock revealed no effects on FA morphology (Supplemental Fig. S1a). Anti-paxillin immunostaining of FA in intact cells, hypotonically shocked cells, and FAs on the substrate after trituration revealed no difference in size and spatial organization (Fig. 1b). Quantifying fluorescence density (intensity/ μm^2) of immunolocalized paxillin, vinculin, zyxin, talin, phospho-tyrosine, and VASP in FAs showed that neither hypotonic shock nor trituration altered their FA abundance compared to intact cells, and no proteins remained on the substrate after FA collection (Supplemental Fig. S1b). We also compared the concentration of FA proteins (paxillin, vinculin, talin, VASP, actin, phosphorylated paxillin, and phosphorylated FAK), soluble (GAPDH), cytoskeletal (tubulin), and membrane-associated components (Akt and FGFR) in isolated FA and cell body fractions by

western blot. This confirmed that the isolation method concentrated FA components in the FA fraction and separated and concentrated soluble, cytoskeletal, and membrane-associated components in the cell body fraction (Fig. 1c). The presence of FA proteins in the cell body fraction agrees with their known localizations to non-FA structures. Therefore, our FA isolation method preserves native FA organization and size and association of known FA proteins.

Proteomic analysis of isolated FAs

Isolated HFF1 FAs were then analyzed by multidimensional protein identification technology mass spectrometry (MudPIT MS)²⁶. FAs were collected, solubilized, denatured, and the abundant proteins actin and fibronectin removed by immunodepletion. Remaining proteins were reduced, alkylated, protease digested and separated by two-dimensional liquid chromatography prior to MS analysis. Tandem mass spectra were generated and matched to peptides in a human protein database using SEQUEST^{TM27}. Each protein is represented by multiple mass spectra (sequence counts) from different peptide fragments, and each peptide fragment can be detected multiple times. Protein abundance was thus quantified as the sum of all mass spectra identified per protein (spectrum counts).

We applied two criteria for considering a protein a reproducibly identified component of isolated FAs (Fig. 2a). To be included in a “detectable list” required presence of one or more sequence count and a false positive protein identification rate of less than 1%²⁸ (Supplemental Methods). Inclusion in the “reproducible list” required inclusion in the detectable list in at least two out of three replicate runs. By these criteria, 1917 and 754 proteins were identified as detectable and reproducible components of isolated FA, respectively (Supplemental Table 1). Although the reproducibly identified proteins may include cytosolic and cytoskeletal contaminants, this first comprehensive analysis of FA composition likely includes many undiscovered FA proteins.

We classified the reproducibly identified proteins in isolated FA according to their cell biological function. Of the 150 proteins in the Integrin Adhesome³, 72 and 50 proteins were identified in our detectable and reproducible lists, respectively. Cell type or ECM composition differences, or protein susceptibility to digestion may underlie our inability to identify all Adhesome proteins. 283 proteins were grouped into an “expected FA list” based on further literature analysis. This included the 50 proteins in the Adhesome as well as proteins in the same family (24), known to interact with (142), or subunits of a macromolecular complex (47) of an Adhesome member, as well as 20 FA associated proteins that were not included in the Adhesome (Fig. 2b). Thus, nearly 40% (283 out of 754 total) of the reproducibly identified proteins could be expected to be present in FAs based on their known properties (Fig. 2c), providing further validation of our FA isolation and protein identification method. We illustrate our FA composition, with an interactome of proteins in our expected FA list (Supplemental Fig. S2), with protein functional classification color-coded and characterized interactions indicated by overlap (Supplemental Table 2 and <http://dir.nhlbi.nih.gov/papers/lctm/focaladhesion/Home/index.html>).

The remaining ~60% (471 out of 754 total) of reproducibly identified proteins in isolated FA (Supplemental Table 3) were either uncharacterized, had no known association with,

function in, or interaction with FAs or proteins in the Adhesome. These may be undiscovered or weakly associated or transient FA proteins, or cytosolic and/or cytoskeletal contaminants. These were classified according to biological function: endomembrane systems/trafficking (129); uncharacterized (84); cytoskeleton (81); metabolism (70); plasma membrane channels/transporters (36); RNA/DNA processing (31); cytosolic signaling (25); or folding/degradation (15). The large proportion of cytoskeletal and endomembrane trafficking proteins is not surprising, given that part of actin stress fibers were isolated with FA, and all three cytoskeletal systems associate with FAs²⁹, while endomembrane trafficking regulates FA turnover³⁰. Similarly, membrane channels are included in the plasma membrane present in FA. However, the purpose of this study is not comprehensive documentation of *bona fide* FA proteins, but rather determination of FA composition changes mediated by myosinII activity.

“MyosinII Dependence Ratio” (MDR) quantifies the myosinII activity-dependence of protein abundance in FAs

We next characterized the effects of myosinII inhibition on protein composition and abundance in isolated FAs. MyosinII activity was inhibited with blebbistatin (50 μ M, 2hr). Immunolocalization of paxillin in intact cells showed that blebbistatin abolished large, central FA and induced small, peripheral FA, with FA of a similar size and spatial distribution remaining substrate-bound after isolation (Fig. 3a,b). MudPIT MS analysis of isolated FA from blebbistatin-treated cells revealed reproducible identification of 665 proteins (Supplemental Table 4), 517 of which (78%) were reproducibly identified in FA of control cells, for a total of 905 proteins from both conditions (237 proteins only in control FAs, 148 proteins only in blebbistatin-treated FAs, and 517 proteins in both conditions).

To evaluate the relative changes in protein abundance in FAs isolated from control and blebbistatin-treated cells, we developed a normalized, ratio-based metric, the “MyosinII Dependence Ratio” (MDR), that represents the dependence of a protein’s abundance in FA on myosinII activity. MDR was the ratio of normalized protein abundance (total spectrum counts) in control FAs to that in FAs from blebbistatin-treated cells (Fig. 3c, Supplemental Methods). Because digestion and detection efficiencies are independent of sample origin, spectrum counts accurately reflect relative change in protein abundance in similarly prepared samples^{31,32}. Thus MDR<1 indicates myosinII activity inhibits the protein’s accumulation in FA, MDR close to 1 indicates myosinII activity-independent FA association, and MDR>1 indicates myosinII activity-dependent enrichment in FA.

We validated MudPIT MS-based MDR results by comparison to western blot and two-dimensional fluorescence difference gel electrophoresis analysis (2D-DIGE)³³. Western analysis (20 different proteins) and 2D-DIGE (21 different proteins) comparison of protein abundance in isolated FA from control and blebbistatin-treated cells revealed corroboration rates of 95% (Supplemental Table 5) and 90% (Supplemental Fig. S3 and Table 6) with MDRs, respectively. Thus, MDR provides a reliable metric for determining how myosinII activity effects relative abundance of proteins in FAs.

MyosinII activity promotes FA accumulation of FA assembly, maturation, and disassembly factors, and FA loss of lamellipodial protrusion factors

To characterize how FA composition is modulated by myosinII activity, proteins were categorized according to their MDR magnitude. Of the 905 reproducibly identified proteins in FA of control and blebbistatin-treated cells, 459 proteins (51%) showed ≥ 2 -fold difference in abundance between conditions. These included 335 proteins with $\text{MDR} > 2$, indicating FA enrichment by myosinII contraction. Surprisingly, 124 proteins exhibited $\text{MDR} < 0.5$, indicating suppression of their FA abundance by myosinII activity (Fig. 4a). Many proteins exhibited changes between 1.25–2-fold ($\text{MDR}: 1.25\text{--}2$ or $0.5\text{--}0.8$). This represents either minor myosinII-dependent changes in FA abundance, or low confidence/low detectability by MudPIT methods. Thus, myosinII activity both positively and negatively effects FA enrichment of proteins to promote major changes in FA composition.

We created a myosinII-responsive FA interactome from proteins in the expected FA list by color-coding proteins according to MDR magnitude (Supplemental Fig. S4 and Table 7, <http://dir.nhlbi.nih.gov/papers/lctm/focaladhesion/Home/index.html>). The interactome illustrates the full range of MDR values, including proteins exhibiting minor/low confidence changes. This interactome suggests how myosinII activity may collectively modulate FA abundance of groups of proteins mediating distinct pathways.

Proteins known to be involved in pathways of myosinII-mediated FA maturation and stress fiber formation were enriched in FA of controls compared to blebbistatin-treated cells (Fig. 4b). This included minor FA enrichment of RhoA⁷ ($\text{MDR}:1.29$) and greater enrichment of enhancers of Rho activity including GEF-H1³⁴ ($\text{MDR}:2.00$), TRIP6³⁵ ($\text{MDR}:3.86$) and testin³⁶ ($\text{MDR}:6.65$). Stress fiber formation regulators enriched in control FAs included the actin bundling proteins α -actinin³⁷ ($\text{MDR}:4.19$), synaptopodin-2³⁸ ($\text{MDR}:2.60$), supervillin^{39,40}, formin-2⁴¹ ($\text{MDR}:1.86$), and several PDZ-LIM cytoskeletal adapters⁴² (zyxin, $\text{MDR}:2.91$; PDLI1, $\text{MDR}:6.77$; PDLI4, $\text{MDR}:2.93$; PDLI5, $\text{MDR}:1.33$; PDLI7, $\text{MDR}:2.11$; and FHL2, $\text{MDR}:2.07$).

MyosinII inhibition also reduced FA abundance of factors mediating integrin-actin linkage^{13,43–45} (Fig. 4c). FA accumulation of migfilin ($\text{MDR}:9.72$) and filamins (filamin-1, $\text{MDR}:2.88$; filamin-B, $\text{MDR}:2.31$; and filamin-C, $\text{MDR}:2.50$) was strongly inhibited by blebbistatin. Blebbistatin also weakly inhibited FA abundance of talin-1 ($\text{MDR}:1.33$) and vinculin ($\text{MDR}:1.41$) and its binding partner, vinexin⁴⁶ ($\text{MDR}:1.59$). Thus, myosinII activity promotes FA accumulation of integrin-cytoskeletal linkers.

Disassembly of mature FA is regulated by calpain-mediated proteolysis⁴⁷ and/or endocytosis of integrins^{30,48}. Components of both of these pathways were strongly enriched in FA from control cells compared to blebbistatin-treated cells. This included calpain-2 and components of both clathrin-dependent (clathrin heavy chain-1, $\text{MDR}:2.08$; clathrin adapters Dab2, $\text{MDR}:2.74$ and numb, $\text{MDR}:1.94$) and caveolin-mediated, clathrin-independent pathways (caveolin-1, $\text{MDR}:2.21$; scaffolding proteins flotillin-1, $\text{MDR}:12$ and flotillin-2 $\text{MDR}:1.48$) (Fig. 4d). This suggests mature FAs recruit disassembly factors by a myosinII-dependent pathway.

Surprisingly, we also found proteins involved in Rac1-mediated lamellipodial protrusion were strongly enriched in FA of blebbistatin-treated cells compared to controls, indicating negative regulation of their FA recruitment by myosinII activity. Although Rac1 (MDR: 2.47) itself was more enriched in FA of control cells, myosinII inhibition caused FA enrichment of Rac1 activators, effectors, and downstream targets (Fig. 4e). Rac1 activators included the Rac guanine nucleotide exchange factor (GEF) β -PIX⁴⁹ (MDR:0.27) and the Rac GEF modulator, EPS8⁵⁰ (MDR:0.48), while PKA⁵¹ and its A-kinase activating protein, MAP2⁵², MIF⁵³, and the RhoA inhibitor RhoGDI⁵⁴ (MDR:0.19) have all my indirectly promote Rac1 activation. Rac1 effectors included IRSP53⁵⁵ and N-WASP^{55,56} (MDR:0.26), both mediators of Arp2/3-dependent actin polymerization. Rac1 downstream targets involved in actin treadmilling included Arp2/3 ((ARC1A (MDR:0.24), ARC1B (MDR: 0.68), ARPC3 (MDR:0.69), ARP5L (MDR:0.74)), cofilin⁵⁷ (MDR:0.46) and its activator PP2A⁵⁸ (MDR:0.21), and the actin monomer binding protein Cap1⁵⁹ (MDR:0.25).

Contractility-mediated FA maturation promotes β -PIX dissociation from nascent FAs

To understand how myosinII activity negatively regulates Rac1 and lamellipodial protrusion, we focused on the Rac GEF β -PIX. Immunoblotting FA fractions validated myosinII's negative regulation of β -PIX accumulation in FA, showing a 3.73-fold concentration of β -PIX in FA by myosinII inhibition compared to control, similar to the MDR (3.7-fold (1/MDR) (Fig. 5a)). Quantifying the ratio of fluorescence density of paxillin and β -PIX in FA showed that myosinII inhibition did not significantly effects paxillin FA density, but significantly increased (25%) FA density of β -PIX compared to control (Fig. 5b,c). β -PIX accumulation in FAs was also regulated by physiological downregulation of myosinII contractility⁶⁰, since western blot of isolated FAs and immunofluorescence analysis revealed increased accumulation of β -PIX in FAs from cells plated on compliant compared to stiffer substrates(Fig. 5d,e,f). Thus, β -PIX concentration in FAs is negatively regulated by myosinII contractility.

To determine if FA maturation modulates FA abundance of β -PIX, we quantified the ratio of fluorescence density in immature ($<2\mu\text{m}^2$) relative to mature ($>2\mu\text{m}^2$) FA. This revealed 9% more paxillin in big compared small to FAs, but 25% less β -PIX (Fig. 5b,c). Analysis of mApple-paxillin and eGFP- β -PIX during FA maturation showed that paxillin and β -PIX concentrations and FA area all increased at similar rates as nascent FA assembled. Subsequently, FA area increase slowed, paxillin continued to accumulate, but β -PIX level did not increase and eventually decreased in large, paxillin-dense FA (Fig. 5g). Analysis of paxillin and β -PIX during perfusion of Y27632 to inhibit ROCK (10 μM ; blebbistatin could not be used due to phototoxicity) revealed that reducing contraction caused dissociation of paxillin and FA shrinkage, concomittant with association of β -PIX, followed by adhesion turnover (Fig. 5h and Supplemental Fig. S5). Thus, β -PIX concentrates in assembling nascent FAs in the absence of myosinII contractility, and it dissociates from FA during myosinII-mediated FA maturation.

β -PIX in nascent FAs induces Rac1 activation, negatively regulates FA maturation and promotes cell migration

We next examined the role of β -PIX in Rac1 activation and lamellipodial formation induced by myosin II inhibition^{61,62}. Immunolocalization of paxillin and the lamellipodia marker, cortactin, in GFP- β -PIX-expressing cells showed that β -PIX localized in nascent FAs in lamellipodia^{63,64} induced by blebbistatin (Fig. 6a). Lentiviral expression of shRNAs to inhibit β -PIX expression abrogated the blebbistatin-induced enhancement of cell spreading and decreased the ratio of lamellipodia area to total cell area⁶⁵ (Fig. 6b and Supplemental Fig. S7). Rac1-GTP pulldown assays revealed that in cells expressing control shRNAs, Rac1 activity was increased by blebbistatin treatment⁶¹ (Fig. 6c), while blebbistatin-induced Rac1 activation was abolished by β -PIX knockdown. This inhibitory effect was not induced by silencing the related FA-associated Rac GEF, α -PIX, and was rescued by re-expressing myc-tagged mouse β -PIX (Fig. 6c, Supplemental Fig. S6). Thus, β -PIX is required for lamellipodial formation, cell shape changes, and Rac1 activity induced by inhibition of myosinII.

To determine the role of β -PIX in FA maturation, we altered β -PIX levels and analyzed FA size. Overexpression of β -PIX abrogated mid-sized (2–6 μm^2) FA, promoted small FA (<2 μm^2) at the cell periphery, and significantly increased the proportion of small FA compared to controls (Fig. 7a,b). In contrast, silencing β -PIX abrogated small peripheral FA and increased mid-sized FA (Fig. 7a,b). Analysis of mApple-paxillin (Fig. 7c) revealed that β -PIX silencing had little effect on FA assembly rate (Fig. 7c) or maximal paxillin level (Fig. 7e), but slowed FA disassembly (Fig. 7c), significantly increasing FA lifetime compared to control (Fig. 7d). Silencing β -PIX also reduced migration velocity compared to controls, and abrogated the enhancement of cell velocity induced by inhibiting myosinII with blebbistatin (Fig. 7f, Supplemental Table 9). Thus, β -PIX drives rapid nascent FA turnover, negatively regulating FA maturation and enhancing cell migration.

DISCUSSION

We developed a proteomics approach to profile global FA composition changes in response to inhibition of myosinII activity to better understand myosinII-driven FA maturation. This method provides a powerful approach for dissecting FA composition changes in response to different stimuli or molecular perturbations²⁵. Our FA proteome contained 905 proteins, supporting the notion that FA are complex organelles. Whether all these proteins participate in FA function is unknown. More importantly, we show that protein abundance of half (459/905) the FA proteome is altered by myosinII activity and half remain constant as core FA components or non-specific contaminants. Most FA compositional change is likely not caused by myosinII ATPase activity acting directly on FA proteins or indicative of protein tension sensitivity *per se*, but reflects downstream effects of myosinII-mediated mechanotransduction. Our results define the myosinII-responsive FA proteome, indicating substantial compositional differences between immature and mature FA. Inhibiting myosinII reduced FA abundance of 73% of the myosinII-responsive FA proteome, supporting the established role of myosinII as an enhancer of FA protein recruitment. However, surprisingly, inhibition of myosinII induced FA enrichment of 27% of the myosinII-

responsive FA proteome, indicating for the first time that myosinII is an important negative regulator of FA protein recruitment.

FA composition in myosinII-inhibited cells likely reflects that in nascent FA that form and turn over rapidly during lamellipodial protrusion in the absence of local myosinII activity^{66,67}, and which are critical to cell migration¹⁷. Though our controls include FA of various maturation states, their FA composition is likely dominated by larger and more abundant matured FA in the lamella and cell center which are disassembling or specialized for ECM remodeling. Whether similar FA compositional changes occur is being investigated.

Our results suggest a model in which myosinII activity regulates FA maturation and turnover by collectively modulating the FA abundance of protein functional modules mediating specialization of FA for cell migration. FA abundance of inside-out integrin activation, (talins, kindlins) was not myosinII-sensitive, supporting the notion that nascent FA formation is contractility-independent¹⁷. Our results suggest that, independent of contractility, activated integrin complexes recruit Rac1 activators (β -PIX, EPS8, MIF, PKA) and Rac1 effectors (IRSP53, N-WASP) and their targets involved in dendritic actin treadmilling (Arp2/3, cofilin-1, CAP-1). This suggests a positive feedback mechanism in which lamellipodial protrusion is coupled to formation of nascent FA that recruit a Rac1 regulatory module which propagates further protrusion and nascent FA formation to drive cell migration.

Nascent FA subjected to myosinII contractility exhibit both dissociation and recruitment of protein functional modules that mediate FA strengthening, stress fiber formation, and mature FA disassembly (Fig. 7g). We find that myosinII promotes enrichment of proteins that strengthen the integrin-actin linkage (migfilin, filamins, vinculin). At the same time, contractility drives FA dissociation of the Rac1 regulatory module to terminate the nascent FA turnover loop and allow FA maturation. MyosinII-driven loss of the Rac1 module is mirrored by recruitment of RhoA, its activators (GEF-H1, TRIP6, testin), and downstream targets and stress fiber proteins including actin-bundling proteins (α -actinin, supervillin, formin-2, and synaptopodin-2) and cytoskeletal adapters (PDLI1, PDLI4, PDLI5, PDLI7, zyxin, and FHL2). Contraction also drives FA disassembly¹⁵ by recruiting calpain and clathrin-dependent and caveolin-mediated endocytosis protein modules..

To support the role of myosinII in negative regulation of a Rac1 regulatory module in FA, we focused on the Rac GEF β -PIX, and examined the myosinII-dependence of its role in nascent FA turnover and lamellipodial protrusion^{63,64}. We find that β -PIX concentrates in nascent FA⁶⁴, and dissociates from FA as they mature. We show that β -PIX is required for Rac1 activity and lamellipodial protrusion induced by myosinII inhibition, suggesting that β -PIX may enhance Rac1 activity locally in myosinII-free cell regions such as lamellipodia. Finally, we show that β -PIX is required for rapid nascent FA turnover, implicating it in negative regulation of FA maturation and enhancement of cell migration.

Supplementary Material

Refer to Web version on PubMed Central for supplementary material.

Acknowledgments

We thank J. Hildebrand (University of Pittsburgh), J. Peterson (Fox Chase Cancer Center), M. Davidson (Florida State), R.H. Chen (Academia Sinica) and M. Beckerle (University of Utah) for reagents, the NHLBI proteomics and flow cytometry facilities, William Shin and Ian Schneider for help with imaging and analysis, and Aaron Aslanian. C.M.W. is supported by NHLBI, J.R.Y. by NIH P41 RR011823.

References

1. Burridge K, Fath K, Kelly T, Nuckolls G, Turner C. Focal adhesions: transmembrane junctions between the extracellular matrix and the cytoskeleton. *Annu Rev Cell Biol.* 1988; 4:487–525. [PubMed: 3058164]
2. Hynes RO. Integrins: bidirectional, allosteric signaling machines. *Cell.* 2002; 110:673–687. [PubMed: 12297042]
3. Zaidel-Bar R, Itzkovitz S, Ma'ayan A, Iyengar R, Geiger B. Functional atlas of the integrin adhesion. *Nat Cell Biol.* 2007; 9:858–867. [PubMed: 17671451]
4. Zamir E, Geiger B, Kam Z. Quantitative multicolor compositional imaging resolves molecular domains in cell-matrix adhesions. *PLoS One.* 2008; 3:e1901. [PubMed: 18382676]
5. Bershadsky A, Kozlov M, Geiger B. Adhesion-mediated mechanosensitivity: a time to experiment, and a time to theorize. *Curr Opin Cell Biol.* 2006; 18:472–481. [PubMed: 16930976]
6. Burridge K, Chrzanowska-Wodnicka M. Focal adhesions, contractility, and signaling. *Annu Rev Cell Dev Biol.* 1996; 12:463–518. [PubMed: 8970735]
7. Chrzanowska-Wodnicka M, Burridge K. Rho-stimulated contractility drives the formation of stress fibers and focal adhesions. *J Cell Biol.* 1996; 133:1403–1415. [PubMed: 8682874]
8. Pletjushkina OJ, et al. Maturation of cell-substratum focal adhesions induced by depolymerization of microtubules is mediated by increased cortical tension. *Cell Adhes Commun.* 1998; 5:121–135. [PubMed: 9638333]
9. Riveline D, et al. Focal contacts as mechanosensors: externally applied local mechanical force induces growth of focal contacts by an mDia1-dependent and ROCK-independent mechanism. *J Cell Biol.* 2001; 153:1175–1186. [PubMed: 11402062]
10. Galbraith CG, Yamada KM, Galbraith JA. Polymerizing actin fibers position integrins primed to probe for adhesion sites. *Science.* 2007; 315:992–995. [PubMed: 17303755]
11. Vogel V, Sheetz M. Local force and geometry sensing regulate cell functions. *Nat Rev Mol Cell Biol.* 2006; 7:265–275. [PubMed: 16607289]
12. Engler AJ, Sen S, Sweeney HL, Discher DE. Matrix elasticity directs stem cell lineage specification. *Cell.* 2006; 126:677–689. [PubMed: 16923388]
13. Tadokoro S, et al. Talin binding to integrin beta tails: a final common step in integrin activation. *Science.* 2003; 302:103–106. [PubMed: 14526080]
14. Laukaitis CM, Webb DJ, Donais K, Horwitz AF. Differential dynamics of alpha 5 integrin, paxillin, and alpha-actinin during formation and disassembly of adhesions in migrating cells. *J Cell Biol.* 2001; 153:1427–1440. [PubMed: 11425873]
15. Webb DJ, et al. FAK-Src signalling through paxillin, ERK and MLCK regulates adhesion disassembly. *Nat Cell Biol.* 2004; 6:154–161. [PubMed: 14743221]
16. Wiseman PW, et al. Spatial mapping of integrin interactions and dynamics during cell migration by image correlation microscopy. *J Cell Sci.* 2004; 117:5521–5534. [PubMed: 15479718]
17. Choi CK, et al. Actin and alpha-actinin orchestrate the assembly and maturation of nascent adhesions in a myosin II motor-independent manner. *Nat Cell Biol.* 2008; 10:1039–1050. [PubMed: 19160484]

18. Pasapera AM, Schneider IC, Rericha E, Schlaepfer DD, Waterman CM. Myosin II activity regulates vinculin recruitment to focal adhesions through FAK-mediated paxillin phosphorylation. *J Cell Biol.* 2010; 188:877–890. [PubMed: 20308429]
19. Galbraith CG, Sheetz MP. A micromachined device provides a new bend on fibroblast traction forces. *Proc Natl Acad Sci U S A.* 1997; 94:9114–9118. [PubMed: 9256444]
20. Huttenlocher A, Ginsberg MH, Horwitz AF. Modulation of cell migration by integrin-mediated cytoskeletal linkages and ligand-binding affinity. *J Cell Biol.* 1996; 134:1551–1562. [PubMed: 8830782]
21. Zaidel-Bar R, Ballestrem C, Kam Z, Geiger B. Early molecular events in the assembly of matrix adhesions at the leading edge of migrating cells. *J Cell Sci.* 2003; 116:4605–4613. [PubMed: 14576354]
22. Friedland JC, Lee MH, Boettiger D. Mechanically activated integrin switch controls alpha5beta1 function. *Science.* 2009; 323:642–644. [PubMed: 19179533]
23. Shi Q, Boettiger D. A novel mode for integrin-mediated signaling: tethering is required for phosphorylation of FAK Y397. *Mol Biol Cell.* 2003; 14:4306–4315. [PubMed: 12960434]
24. Ballestrem C, et al. Molecular mapping of tyrosine-phosphorylated proteins in focal adhesions using fluorescence resonance energy transfer. *J Cell Sci.* 2006; 119:866–875. [PubMed: 16478788]
25. Kuo, JC.; Han, X.; Yates, JR.; Waterman, CM. Isolation of focal adhesion proteins for biochemical and proteomic analysis. In: Shimaoka, Motomu, editor. “Integrin and Cell Adhesion Molecules: Methods and Protocols” *Methods in Molecular Biology.* Humana Press; 2010. Ref Type: In Press
26. Washburn MP, Wolters D, Yates JR III. Large-scale analysis of the yeast proteome by multidimensional protein identification technology. *Nat Biotechnol.* 2001; 19:242–247. [PubMed: 11231557]
27. Eng JK, McCormack AL, Yates JR III. An approach to correlate tandem mass spectral data of peptides with amino acid sequences in a protein database. *J Am Soc Mass Spectrom.* 94 A.D; 5:976–989. [PubMed: 24226387]
28. Elias JE, Haas W, Faherty BK, Gygi SP. Comparative evaluation of mass spectrometry platforms used in large-scale proteomics investigations. *Nat Methods.* 2005; 2:667–675. [PubMed: 16118637]
29. Zaidel-Bar R, Geiger B. The switchable integrin adhesome. *J Cell Sci.* 2010; 123:1385–1388. [PubMed: 20410370]
30. Caswell PT, Vadrevu S, Norman JC. Integrins: masters and slaves of endocytic transport. *Nat Rev Mol Cell Biol.* 2009; 10:843–853. [PubMed: 19904298]
31. Liu H, Sadygov RG, Yates JR III. A model for random sampling and estimation of relative protein abundance in shotgun proteomics. *Anal Chem.* 2004; 76:4193–4201. [PubMed: 15253663]
32. Paoletti AC, et al. Quantitative proteomic analysis of distinct mammalian Mediator complexes using normalized spectral abundance factors. *Proc Natl Acad Sci U S A.* 2006; 103:18928–18933. [PubMed: 17138671]
33. Marouga R, David S, Hawkins E. The development of the DIGE system: 2D fluorescence difference gel analysis technology. *Anal Bioanal Chem.* 2005; 382:669–678. [PubMed: 15900442]
34. Ren Y, Li R, Zheng Y, Busch H. Cloning and characterization of GEF-H1, a microtubule-associated guanine nucleotide exchange factor for Rac and Rho GTPases. *J Biol Chem.* 1998; 273:34954–34960. [PubMed: 9857026]
35. Bai CY, Ohsugi M, Abe Y, Yamamoto T. ZRP-1 controls Rho GTPase-mediated actin reorganization by localizing at cell-matrix and cell-cell adhesions. *J Cell Sci.* 2007; 120:2828–2837. [PubMed: 17652164]
36. Griffith E, Coutts AS, Black DM. RNAi knockdown of the focal adhesion protein TES reveals its role in actin stress fibre organisation. *Cell Motil Cytoskeleton.* 2005; 60:140–152. [PubMed: 15662727]
37. Otey CA, Carpen O. Alpha-actinin revisited: a fresh look at an old player. *Cell Motil Cytoskeleton.* 2004; 58:104–111. [PubMed: 15083532]
38. Schroeter MM, Beall B, Heid HW, Chalovich JM. In vitro characterization of native mammalian smooth-muscle protein synaptopodin 2. *Biosci Rep.* 2008; 28:195–203. [PubMed: 18588515]

39. Chen Y, et al. F-actin and myosin II binding domains in supervillin. *J Biol Chem.* 2003; 278:46094–46106. [PubMed: 12917436]
40. Wulfkuhle JD, et al. Domain analysis of supervillin, an F-actin bundling plasma membrane protein with functional nuclear localization signals. *J Cell Sci.* 1999; 112 (Pt 13):2125–2136. [PubMed: 10362542]
41. Schuh M, Ellenberg J. A new model for asymmetric spindle positioning in mouse oocytes. *Curr Biol.* 2008; 18:1986–1992. [PubMed: 19062278]
42. Harris BZ, Lim WA. Mechanism and role of PDZ domains in signaling complex assembly. *J Cell Sci.* 2001; 114:3219–3231. [PubMed: 11591811]
43. Meves A, Stremmel C, Gottschalk K, Fassler R. The Kindlin protein family: new members to the club of focal adhesion proteins. *Trends Cell Biol.* 2009; 19:504–513. [PubMed: 19766491]
44. Shattil SJ, Kim C, Ginsberg MH. The final steps of integrin activation: the end game. *Nat Rev Mol Cell Biol.* 2010; 11:288–300. [PubMed: 20308986]
45. Tu Y, Wu S, Shi X, Chen K, Wu C. Migfilin and Mig-2 link focal adhesions to filamin and the actin cytoskeleton and function in cell shape modulation. *Cell.* 2003; 113:37–47. [PubMed: 12679033]
46. Takahashi H, et al. Role of interaction with vinculin in recruitment of vinxins to focal adhesions. *Biochem Biophys Res Commun.* 2005; 336:239–246. [PubMed: 16126177]
47. Franco SJ, et al. Calpain-mediated proteolysis of talin regulates adhesion dynamics. *Nat Cell Biol.* 2004; 6:977–983. [PubMed: 15448700]
48. Ezratty EJ, Bertaux C, Marcantonio EE, Gundersen GG. Clathrin mediates integrin endocytosis for focal adhesion disassembly in migrating cells. *J Cell Biol.* 2009; 187:733–747. [PubMed: 19951918]
49. ten Klooster JP, Jaffer ZM, Chernoff J, Hordijk PL. Targeting and activation of Rac1 are mediated by the exchange factor beta-Pix. *J Cell Biol.* 2006; 172:759–769. [PubMed: 16492808]
50. Innocenti M, et al. Mechanisms through which Sos-1 coordinates the activation of Ras and Rac. *J Cell Biol.* 2002; 156:125–136. [PubMed: 11777939]
51. O'Connor KL, Mercurio AM. Protein kinase A regulates Rac and is required for the growth factor-stimulated migration of carcinoma cells. *J Biol Chem.* 2001; 276:47895–47900. [PubMed: 11606581]
52. Zhong H, et al. Subcellular dynamics of type II PKA in neurons. *Neuron.* 2009; 62:363–374. [PubMed: 19447092]
53. Rendon BE, et al. Regulation of human lung adenocarcinoma cell migration and invasion by macrophage migration inhibitory factor. *J Biol Chem.* 2007; 282:29910–29918. [PubMed: 17709373]
54. Del Pozo MA, et al. Integrins regulate GTP-Rac localized effector interactions through dissociation of Rho-GDI. *Nat Cell Biol.* 2002; 4:232–239. [PubMed: 11862216]
55. Miki H, Yamaguchi H, Suetsugu S, Takenawa T. IRSp53 is an essential intermediate between Rac and WAVE in the regulation of membrane ruffling. *Nature.* 2000; 408:732–735. [PubMed: 11130076]
56. Eden S, Rohatgi R, Podtelejnikov AV, Mann M, Kirschner MW. Mechanism of regulation of WAVE1-induced actin nucleation by Rac1 and Nck. *Nature.* 2002; 418:790–793. [PubMed: 12181570]
57. Oser M, Condeelis J. The cofilin activity cycle in lamellipodia and invadopodia. *J Cell Biochem.* 2009; 108:1252–1262. [PubMed: 19862699]
58. Ambach A, et al. The serine phosphatases PP1 and PP2A associate with and activate the actin-binding protein cofilin in human T lymphocytes. *Eur J Immunol.* 2000; 30:3422–3431. [PubMed: 11093160]
59. Bertling E, et al. Cyclase-associated protein 1 (CAP1) promotes cofilin-induced actin dynamics in mammalian nonmuscle cells. *Mol Biol Cell.* 2004; 15:2324–2334. [PubMed: 15004221]
60. Pelham RJ Jr, Wang Y. Cell locomotion and focal adhesions are regulated by substrate flexibility. *Proc Natl Acad Sci U S A.* 1997; 94:13661–13665. [PubMed: 9391082]

61. Even-Ram S, et al. Myosin IIA regulates cell motility and actomyosin-microtubule crosstalk. *Nat Cell Biol.* 2007; 9:299–309. [PubMed: 17310241]
62. Vicente-Manzanares M, Zareno J, Whitmore L, Choi CK, Horwitz AF. Regulation of protrusion, adhesion dynamics, and polarity by myosins IIA and IIB in migrating cells. *J Cell Biol.* 2007; 176:573–580. [PubMed: 17312025]
63. Koh CG, Manser E, Zhao ZS, Ng CP, Lim L. Beta1PIX, the PAK-interacting exchange factor, requires localization via a coiled-coil region to promote microvillus-like structures and membrane ruffles. *J Cell Sci.* 2001; 114:4239–4251. [PubMed: 11739656]
64. Nayal A, et al. Paxillin phosphorylation at Ser273 localizes a GIT1-PIX-PAK complex and regulates adhesion and protrusion dynamics. *J Cell Biol.* 2006; 173:587–589. [PubMed: 16717130]
65. Lee CS, Choi CK, Shin EY, Schwartz MA, Kim EG. Myosin II directly binds and inhibits Dbl family guanine nucleotide exchange factors: a possible link to Rho family GTPases. *J Cell Biol.* 2010; 190:663–674. [PubMed: 20713598]
66. Desmarais V, Ichetovkin I, Condeelis J, Hitchcock-DeGregori SE. Spatial regulation of actin dynamics: a tropomyosin-free, actin-rich compartment at the leading edge. *J Cell Sci.* 2002; 115:4649–4660. [PubMed: 12415009]
67. Ponti A, Machacek M, Gupton SL, Waterman-Storer CM, Danuser G. Two distinct actin networks drive the protrusion of migrating cells. *Science.* 2004; 305:1782–1786. [PubMed: 15375270]

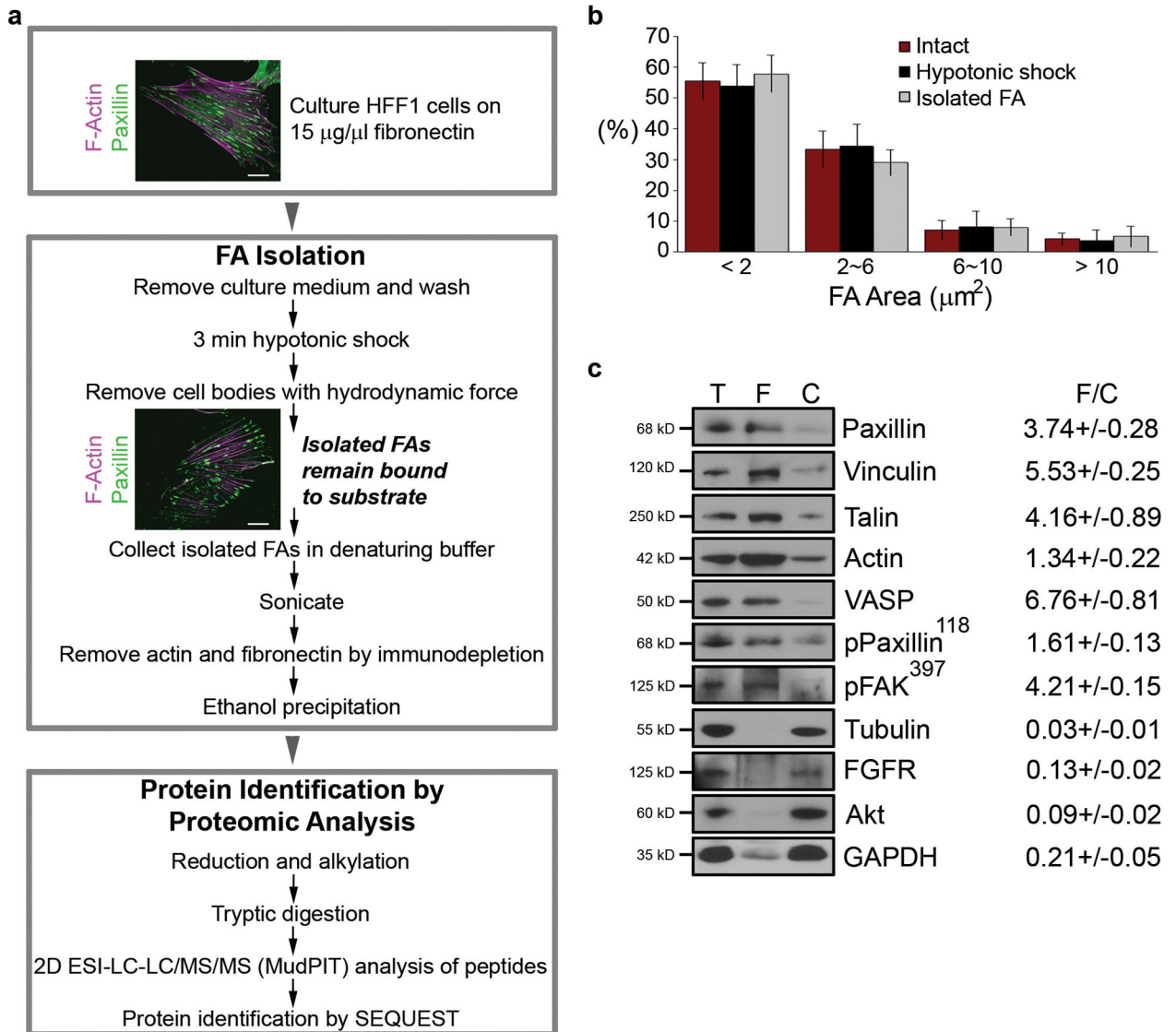


Fig. 1. Development and validation of the FA isolation method

(a) Flow diagram for FA isolation from HFF1 cells and preparation for compositional identification by proteomic analysis. Intact HFF1 cells (top panel) and isolated HFF1 FAs (middle panel) that were immunostained to localize paxillin as an FA marker and F-actin (phalloidin). Scale bars = 20 μm . (b) Histogram of the size distribution of segmented paxillin-containing FA from images of intact cells ($n = 7$ cells 1219 FA), hypototically shocked cells ($n = 7$ cells 944 FA), and isolated FA ($n = 9$ cells, 1217 FA). Bars show SD. No significant differences were detected in the percentage of FA in each size range between FA in these three samples (native: $2.91\pm 0.29\mu\text{m}^2$, hypotonic shock: $2.90\pm 0.82\mu\text{m}^2$, isolated: $2.94\pm 0.57\mu\text{m}^2$). (c) Western blot comparison of protein concentration in total cell lysate (T), isolated FA fractions (F) (before immunodepletion) and cell body fractions (C) (equal total protein was loaded in each lane). The ratio shown on the right (F/C) ($n = 3\sim 4$ experiments, \pm SD) indicates the relative concentration of protein compared between

isolated FA fractions: cell body fractions. Note that this does not reflect the absolute amount of protein in isolated FA fractions and cell body fractions.

Author Manuscript

Author Manuscript

Author Manuscript

Author Manuscript

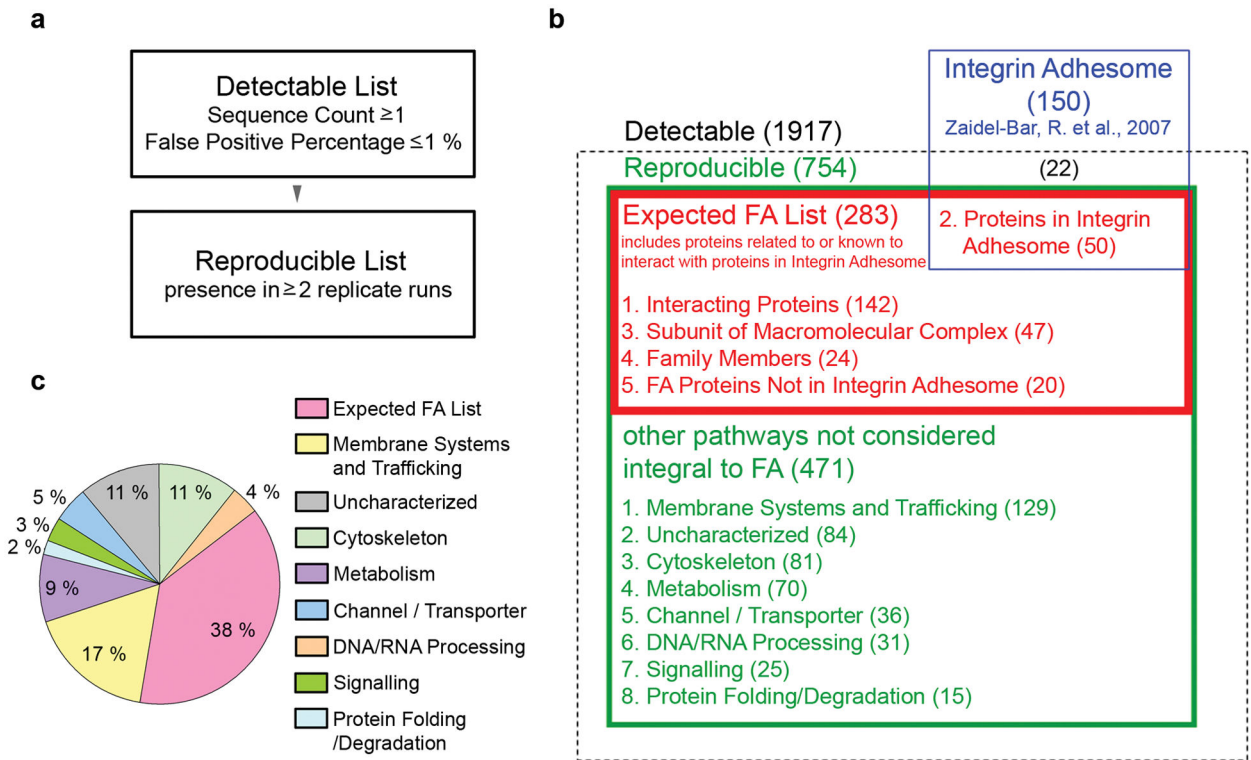


Fig. 2. Proteome of isolated FAs

(a) Criteria applied to data from MudPIT MS analysis for assembling the detectable and reproducible lists of proteins present in isolated FA. (b) Venn diagram and classification of proteins identified in isolated FAs. Number of proteins in each class shown in parentheses. (c) Pie diagram showing the percentage of proteins from the reproducible list categorized according to function.

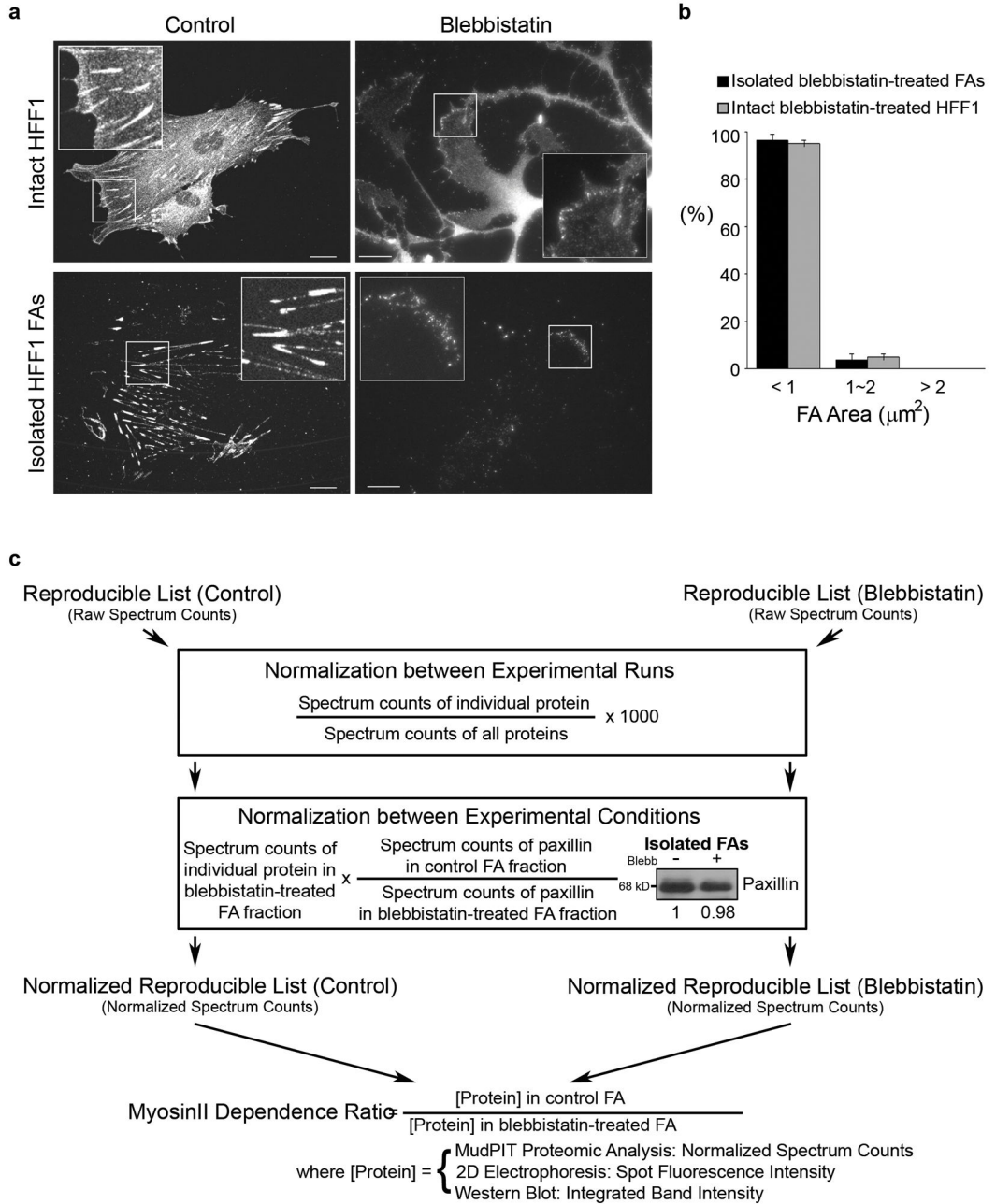


Fig. 3. Development of the MyosinII Dependence Ratio to characterize the effects of myosinII inhibition on protein abundance in isolated FA

(a) Effects of myosinII inhibition by blebbistatin treatment (50 μM , 2h) on the organization and morphology of FAs from intact cells or isolated FAs, visualized by immunostaining for paxillin. Scale bars = 20 μm . (b) Histogram of the size distribution of segmented paxillin-containing FAs from images of intact blebbistatin-treated HFF1 cells (n = 3 cells 526 FAs) and isolated blebbistatin-treated FAs (n = 4 cells 252 FAs). Bars show SD. No significant differences were detected in the percentage of FAs in each size range between FAs from intact cells and isolated FAs. (c) Diagram of the procedure for calculating the MyosinII

Dependence Ratio, representing the change in protein abundance in isolated FA between control and blebbistatin-treated cells.

Author Manuscript

Author Manuscript

Author Manuscript

Author Manuscript

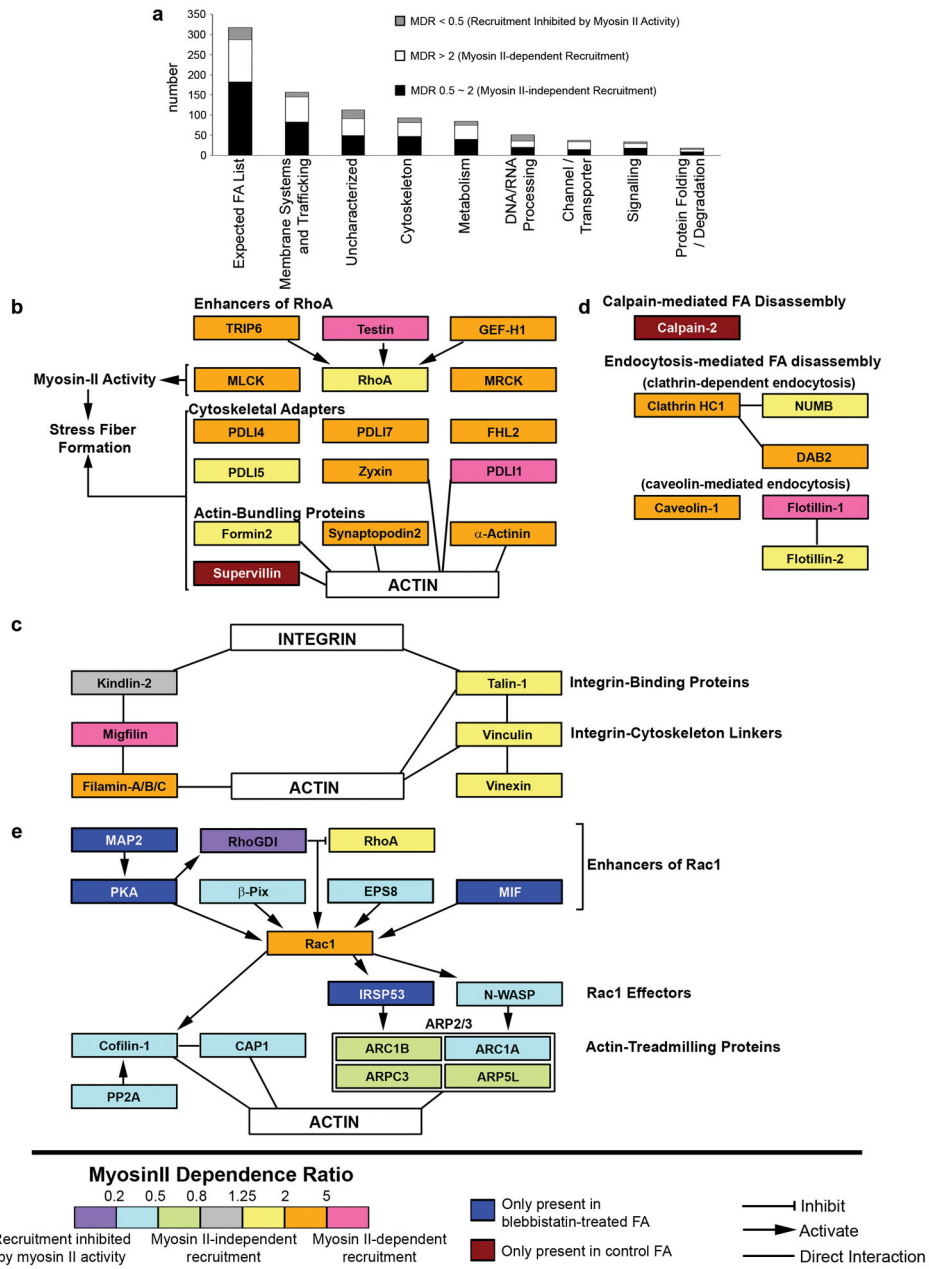


Fig. 4. Collective modulation by myosinII of the FA abundance of proteins in common biological pathways

(a) Number of proteins in different functional categories that exhibit change in abundance (relative to control) in isolated FA in response to blebbistatin treatment. Two-fold differences in abundance (MyosinII Dependence Ratio (MDR) <0.5 or >2) were considered high-confidence significant changes. (b)~(e) Proteins are represented by boxes that are color-coded according to the magnitude of their MyosinII Dependence Ratio (MDR) as in Supplemental Fig. S4. (b) MyosinII-mediated FA enrichment of proteins involved in FA maturation and stress fibers. (c) MyosinII modulation of FA proteins mediating integrin activation and actin linkage. (d) MyosinII-mediated FA enrichment of proteins involved in

calpain-dependent and endocytosis-dependent FA disassembly (e) MyosinII-mediated FA reduction of proteins involved in Rac1 activation and lamellipodial actin treadmilling.

Author Manuscript

Author Manuscript

Author Manuscript

Author Manuscript

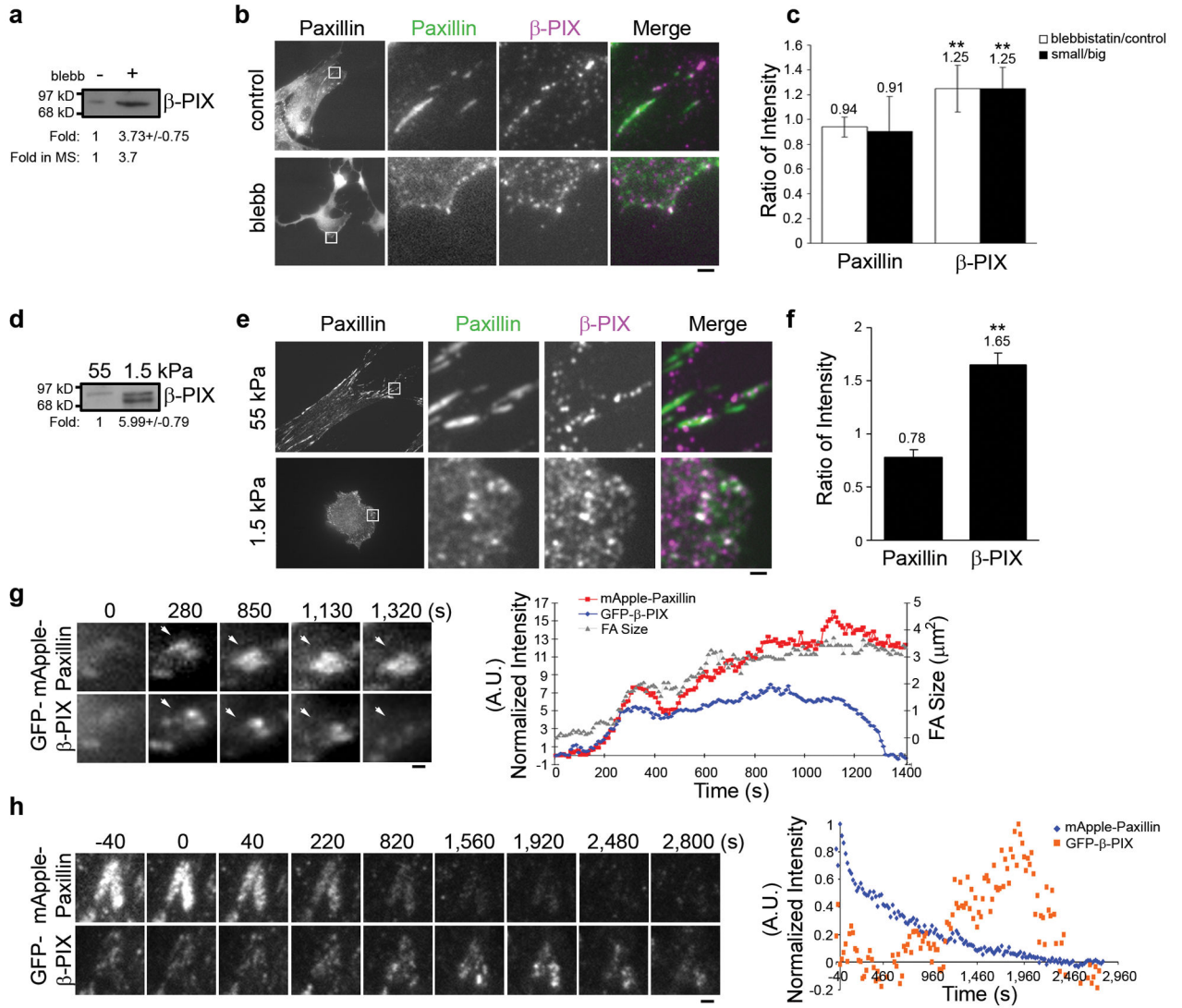


Fig. 5. FA abundance of β-PIX is negatively regulated by myosinII-mediated maturation
 (a) Western blot of isolated FA fractions from control and 50µM blebbistatin-treated cells (equal total protein loaded) with β-PIX antibodies. Fold enrichment in isolated FAs determined by western blot (Fold, n= 3 experiments, +/-SD) or MudPIT MS analysis (Fold in MS) indicated below. (b) TIRF images of immunolocalized paxillin (green) and β-PIX (purple) in control and 50µM blebbistatin-treated (blebb) cells. 6.5µm × 6.5µm boxed regions in left columns are magnified in the right three columns, scale bar = 1µm. (c) Ratio of average density of paxillin or β-PIX immunofluorescence signal (intensity/µm²) within segmented FAs of blebbistatin-treated relative to control cells (blebbistatin/control) or small (<2µm²) relative to big (>2µm²) FAs in control cells (small/big). n = 9 blebbistatin-treated cells, 9 control cells, Bars show SD, **, p<0.05. (d) Western blot with β-PIX antibodies of isolated FA fractions from cells plated on 1.5kPa and 55kPa substrates (equal total protein loaded). Fold enrichment in isolated FAs determined by western blot (Fold, n= 3 experiments, +/-SD) indicated below. (e) Images of immunolocalized paxillin (green) and β-PIX (purple) in cells plated on 1.5kPa and 55kPa substrates. 6.5µm × 6.5µm boxed regions

in left columns are magnified in the right three columns, scale bar = 1 μ m. (f) Ratio of average density of paxillin or β -PIX immunofluorescence signal (intensity/ μ m²) within segmented FAs of cells plated on 1.5kPa relative to 55kPa. n = 6 cells plated on 1.5kPa substrates, 6 cells plated on 55kPa substrates, Bars show SD, **, p<0.05. (g) (left) Images from time-lapse dual-color TIRF series of eGFP- β -PIX and mApple-Paxillin. Time in seconds, scale bar = 1 μ m. (right) Normalized integrated fluorescence intensity (mApple-paxillin, red; eGFP- β -PIX, blue) and FA size (gray) over time in the FA marked with the arrow. (h) (left) Images from a time-lapse dual-color TIRF series of eGFP- β -PIX and mApple-paxillin during perfusion (at time= 0s) of Y27632 (10 μ M) to inhibit ROCK-mediated myosinII activity. Blebbistatin could not be used because of its phototoxic effects in the presence of blue light. Time in seconds. Scale bar = 1 μ m. (right) Normalized integrated fluorescence intensity (mApple-paxillin, blue; eGFP- β -PIX, orange) over time in the FAs in the boxed region.

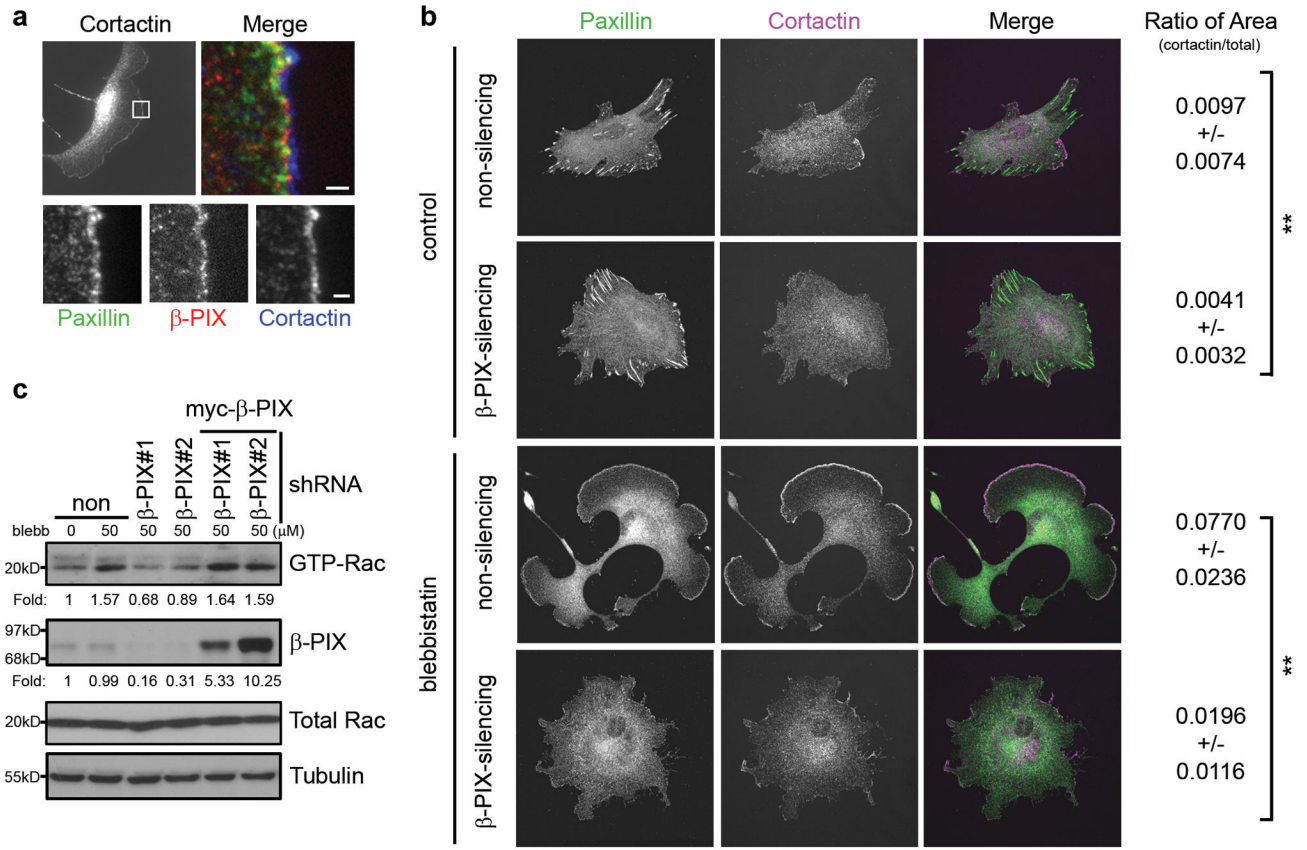


Fig. 6. Effects of β -Pix on regulation of lamellipodia formation and Rac1 activation

(a) GFP- β -PIX (red)-overexpressing HFF1 cells in treatment of 50 μ M blebbistatin (2h) were immunostained for paxillin to localize nascent FA (green) and cortactin to localize protruding lamellipodia (blue). 6 μ m x 6 μ m boxed regions in left columns are magnified in the right and bottom three columns, scale bar = 1 μ m. (b) Cortactin (purple) and paxillin (green) immunostaining of HFF1 cells expressing non-silencing or β -PIX-silencing shRNA (same as β -PIX#1 in c) were treated with 50 μ M blebbistatin (blebbistatin) or not (control). Scale bar = 20 μ m. Right column shows ratio of cortactin-stained cell area relative to total cell area for cells under conditions described above. n=10 cells, +/-SD. **, p<0.05. (c) Effects of β -PIX-silencing on blebbistatin-induced Rac1 activation. HFF1 cells expressing non-silencing (non) or β -PIX-silencing shRNA (β -PIX#1 and β -PIX#2 indicate different sequence targets of β -Pix shRNA) alone or together with myc-tagged mouse β -Pix (myc- β -PIX) were treated with 50 μ M blebbistatin for 2 hr (blebb) or not and cell lysates prepared. Level of GTP-bound Rac1 (GTP-Rac) isolated from lysates by GST-PAK-CRIB pull-down was detected by western blot. Protein level of Rac1 (Total Rac), β -PIX and tubulin in the input lysate detected by western blot. Change relative to control in levels of GTP-Rac and β -PIX determined by western blot (Fold) indicated below.

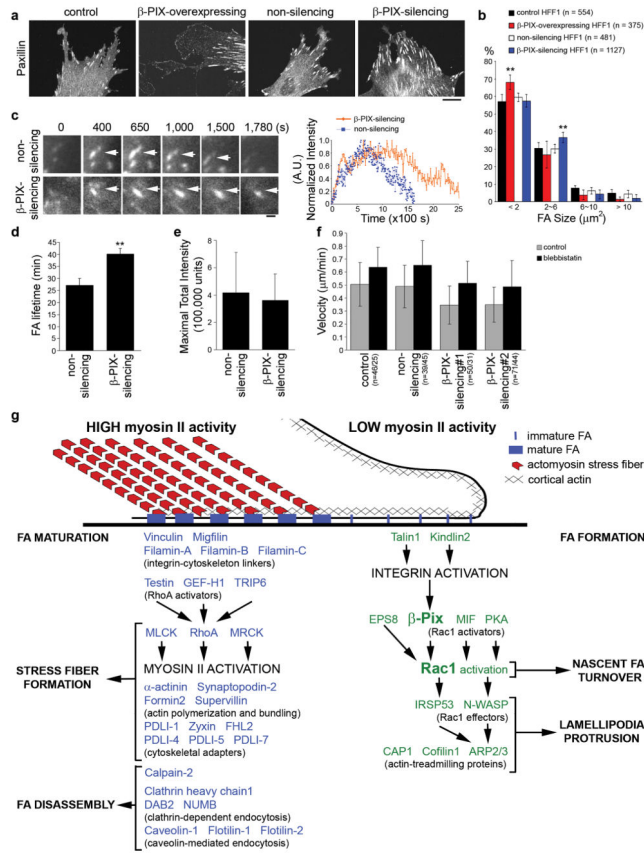


Fig. 7. Effects of β-PIX on FA dynamics and cell migration

(a) Paxillin immunostaining of FAs in control, GFP-β-Pix-overexpressing, non-silencing shRNA-expressing, or β-Pix-silencing (same as β-PIX#1 in Fig. 7c) shRNA-expressing cells. Scale bar = 20 μm. (b) Histogram of size distribution of segmented FAs in the periphery (within 15μm for the cell edge) under conditions described in (a). n= number of FAs. Bars show SD. **, p<0.05. (c) (left) Images from a time-lapse TIRF series of mApple-paxillin during FA turnover in a migrating cell that was expressing non-silencing or β-Pix-silencing (same as β-PIX#1 in Fig. 7c) shRNAs. Scale bar = 1 μm. (right) Normalized fluorescent paxillin intensity over time in the FAs highlighted with arrows. (d) Mean FA lifetime (β-Pix silenced: 40.19±2.38min, control: 27.11±3.00min) and (e) maximal total intensity of mApple-paxillin in FAs under conditions described in (c) (in d and e, non-silencing: n = 19 FAs/5 cells; β-Pix-silencing: n = 15 FAs/6 cells, bars show SD), **, p<0.05. (f) Migration velocity of cells expressing either non-silencing or β-Pix-silencing HFF1 shRNAs with or without 50 μM blebbistatin treatment. n=number of control cells/number of blebbistatin-treated cells, bars show SD. (g) Model of the effects of myosinII contractility on the composition and function of FAs in the leading edge.